

The structure of the saddle point is shown in Figure 7 with the unique normal mode of vibration having an imaginary frequency. The vibration describes well the formations of benzvalene, if one follows the direction of the arrows of vibration in Figure 7, and benzene, if one imagines the reverse directions of the arrows. The changes of atomic distances following the rearomatization are shown in Figure 6b. Starting from benzvalene on the IRC route, the structural change appears in the C<sub>1</sub>-C<sub>3</sub> bond dissociation at first. Thus, the molecule does not hold any of the C<sub>s</sub> or C<sub>2</sub> symmetry overall on the IRC route from benzvalene to benzene. Although the thermal isomerization appears to be a one-step reaction on the S<sub>0</sub> potential energy hypersurface of Figure 6a, precise examination of the bond lengths of Figure 6b reveals that the reaction proceeds in two steps.

In contrast to the IRC on the T<sub>1</sub> hypersurface, the IRC on the S<sub>0</sub> hypersurface does not go through the point corresponding to the prefulvene structure. The point nearest to prefulvene on the S<sub>0</sub> hypersurface is shown as M in Figure 6a, where the C<sub>1</sub>-C<sub>3</sub> bond is fully loosened and the C<sub>2</sub>-C<sub>6</sub> bond is as tight as prefulvene. The prefulvene structure is not a minimum on the S<sub>0</sub> hypersurface, and the steepest descent path from the prefulvene structure leads directly to benzene.

The rearomatization of benzvalene may proceed mainly through the IRC route shown in Figure 6a. So, prefulvene will not be produced in the thermolysis of benzvalene. Because of the singlet-triplet intersection around the prefulvene structure, a chem-

iluminescence is expected if prefulvene is produced in the rearomatization path from benzvalene to benzene. In the analogous rearomatization of Dewar benzene to benzene,<sup>12,13</sup> an energy transfer from triplet-state benzene, which is produced in the thermolysis, to 9,10-dibromoanthracene was followed by the fluorescence of the latter.<sup>14</sup> Turro et al.,<sup>15</sup> however, reported that no chemiluminescence was observed in the thermolysis of benzvalene.

**Acknowledgment.** The authors thank the Computer Center, Institute for Molecular Science, Okazaki, for the use of the M-200H computer and the Library program IMSPAK. The computation was carried out, in considerable part, at the Computer Centre, the University of Tokyo, and the Computer Center, Chiba University. This work was supported in part by Grant in Aid for Scientific Research No. 58209009 from the Ministry of Education, Science and Culture.

Registry No. 1, 81181-42-2; benzene, 71-43-2; benzvalene, 659-85-8.

(12) M. J. S. Dewar, S. Kirschner, and H. W. Kollman, *J. Am. Chem. Soc.*, **96**, 7579 (1974).

(13) M. Tsuda, S. Oikawa, and K. Kimura, *Int. J. Quantum Chem.*, **18**, 157 (1980).

(14) N. J. Turro, P. Lechtken, G. Schuster, J. Orell, H. C. Steinmetzer, W. Adam, *J. Am. Chem. Soc.*, **96**, 1627 (1974).

(15) N. J. Turro, C. A. Renner, T. J. Katz, K. B. Wiberg, and H. A. Connon, *Tetrahedron Lett.*, **46**, 4133 (1976).

## Partitioning of Orbital Framework in Dibenzotetracene Dianion: Manifestation of the Role of Antiaromaticity in 4nπ Conjugated Systems

Abraham Minsky and Mordecai Rabinovitz\*

Contribution from the Department of Organic Chemistry, The Hebrew University of Jerusalem, Jerusalem 91904, Israel. Received December 27, 1983

**Abstract:** The twofold reduction of dibenzotetracene (**1**) to its corresponding dianion was performed with lithium and sodium metals. The resultant doubly charged species revealed unusual <sup>1</sup>H NMR patterns which indicate the existence of a partitioning of the MO's framework of 1<sup>2-</sup> into two parts: "anthracene"-like and "phenanthrene"-like systems, each system exhibiting independent characteristic features, similar to those observed in anthracene and phenanthrene dianions. This mode of partitioning of the condensed system as well as features revealed by the 9-(9'-phenanthryl)anthracene (**4**) tetraanion seem to be an outcome of the imposed antiaromatic contributions.

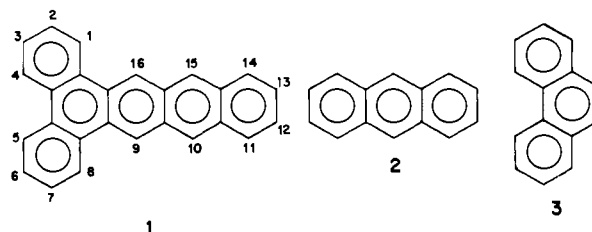
The term "aromaticity" represents a basic, inherent difficulty related to the fact that the aromatic character is not physically observable and hence cannot be directly expressed by measurable data. Still, the notion of aromaticity serves a useful purpose as it enables a general interpretation of a large variety of structural, chemical, and physical phenomena.

The hurdles to be passed in a discussion of the concept of antiaromaticity are even higher, as the experimental data related to the antiaromatic character are quite limited. In principle, cyclic or polycyclic conjugated systems of 4nπ electrons in their peripheral path of conjugation are expected to reveal antiaromatic contribution.<sup>1</sup> Yet, in most cases these contributions, being unfavored in terms of Hückel's rule, are minimized by various mechanisms which reduce the efficiency of the 4nπ electron cyclic delocalization. Antiaromaticity as well as the mechanisms which act to quench its manifestation may account for some highly

unexpected phenomena which occur in systems where the antiaromatic property is imposed by virtue of the "anti-Hückeloid" number of π electrons. This contribution is concerned with the crucial roles which antiaromaticity seems to display in 4nπ conjugated polycycles, a role vividly demonstrated by these phenomena.

### Results and Discussion

**Dibenzotetracene (1) Dianion.** The reduction of dibenzotetracene (**1**) to its corresponding hitherto unknown dianion was performed by lithium and sodium metals. The deep purple

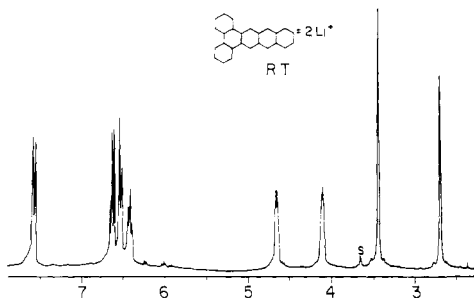


(1) (a) Breslow, R. *Acc. Chem. Res.* **1973**, *6*, 393-398. (b) Haddon, R. C.; Haddon, V. R.; Jackman, L. M. *Fortschr. Chem. Forsch.* **1970**, *16*, 103-220. (c) Cox, R. H.; Terry, H. W.; Harrison, L. W. *Tetrahedron Lett.* **1971**, *50*, 4815-4818.

**Table I.**  $^{13}\text{C}$  NMR Chemical Shifts and Theoretical Parameters of Dibenzotetracene Dianion (as Dilithium Salt)

	C <sub>1</sub>	C <sub>2</sub>	C <sub>3</sub>	C <sub>4</sub>	C <sub>4a</sub>	C <sub>8a</sub>	C <sub>8b</sub>	C <sub>9</sub>	C <sub>10</sub>	C <sub>11</sub>	C <sub>12</sub>	C <sub>9a</sub>	C <sub>10a</sub>
$\delta^a$	152.4	126.5	123.7	146.8	119.5	122.3	116.7	89.0	86.9	112.8	117.6	130.3	126.0
$\psi^b$	0.982	1.113	1.113	1.027	1.056	1.007	0.980	1.324	1.365	1.161	1.120	0.844	0.906
HOMO <sup>c</sup> coeff	0.041	0.141	0.127	0.057	0.184	0.195	0.155	0.362	0.367	0.237	0.173	0.024	0.099
LUMO <sup>d</sup> coeff	0.300	0.351	0.020	0.273	0.278	0.184	0.168	0.032	0.147	0.155	0.081	0.131	0.033

<sup>a</sup>Chemical shifts (ppm) referred to  $\text{SiMe}_4$ . For numbering see scheme. <sup>b</sup>Charge densities as deduced from SCF-MO calculations.<sup>3</sup> <sup>c</sup>Atomic orbital coefficients of the dianion HOMO. <sup>d</sup>Atomic orbital coefficients of the dianion LUMO.

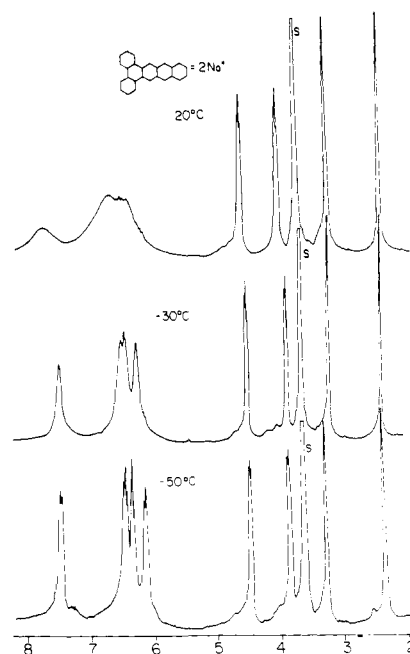
**Figure 1.**  $^1\text{H}$  NMR spectrum of  $1^{2-}$  as dilithium salt.

solution obtained after 6 days of exposure of a THF solution of **1** to lithium wire revealed a highly resolved  $^1\text{H}$  NMR spectrum assigned to the doubly charged species  $1^{2-}$  (Figure 1). The spectrum is composed of two, clearly distinct, components. One group of  $^1\text{H}$  NMR absorptions appears at a relatively low field and consists of a doublet at 7.64 ppm assigned to  $\text{H}_1$  and  $\text{H}_8$  along with a multiplet at 6.43–6.72 ppm which is assigned to protons  $\text{H}_{2,3,4}$  ( $\text{H}_{5,6,7}$ ). The second group of bands attributed to protons  $\text{H}_{9-16}$  appears at a considerably higher field (2.70, s,  $\text{H}_{10,15}$ ; 3.45, s,  $\text{H}_{9,16}$ ; 4.12,  $\text{H}_{11,14}$ , and 4.68,  $\text{H}_{12,13}$ , AA'BB' pattern).

The  $^1\text{H}$  NMR spectrum of  $1^{2-}$  suggests a rather unusual mode of charge density distribution over the dianion, i.e., a formal partitioning of the conjugated doubly charged system into two components: (a) a "phenanthrene" moiety composed of the carbon atoms  $\text{C}_{1-8}$ ,  $\text{C}_{4a,b}$ , and  $\text{C}_{8a,b}$ , as well as  $\text{C}_{16a,b}$ —in terms of the shielding parameters derived from the  $^1\text{H}$  NMR spectrum,<sup>2</sup> this component seems to accommodate only a minor fraction of the overall negative charge density; (b) an "anthracene" moiety which includes all the other carbon atoms along with  $\text{C}_{8b}$  and  $\text{C}_{16a}$  which are shared by the two components—the  $^1\text{H}$  NMR absorptions revealed by the protons attached to this moiety are paratropically shifted, indicating that most of the negative charge density resides over the carbon atoms which constitute the so-called "anthracene" component.<sup>2</sup>

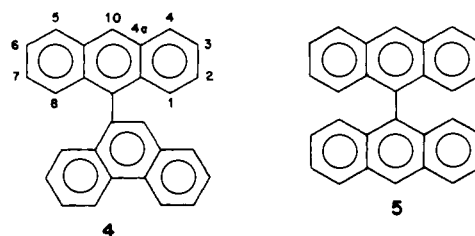
This depiction of charge partitioning is strengthened by  $^{13}\text{C}$  NMR as well as by theoretical calculations (SCF-MO method,<sup>3</sup> Table I). Both experimental and theoretical methods indicate a substantial localization of the negative charge density over those carbons which constitute the "anthracene" moiety. While such a mode of charge distribution is a characteristic feature of nonalternant systems (viz., azulene), it seems rather peculiar when pure benzenoid species are considered. It should be noted that neither the  $^1\text{H}$  NMR nor the  $^{13}\text{C}$  NMR spectra of  $1^{2-}$  as a lithium salt revealed any temperature dependence in the range of  $-50$  to  $+40$  °C.

The  $^1\text{H}$  NMR patterns exhibited by  $1^{2-}$  as a disodium salt are strikingly different from those revealed by the dilithium system and by far more conspicuous (Figure 2). Instead of the two groups of narrow highly resolved absorptions, the  $^1\text{H}$  NMR spectrum of  $1^{2-}$  as disodium salt, recorded at room temperature, reveals only one group of signals. These signals are found to be similar both in chemical shifts and in patterns to the high-field  $^1\text{H}$  NMR bands revealed by the dilithium salt of  $1^{2-}$  i.e., the group assigned to

**Figure 2.**  $^1\text{H}$  NMR spectrum of  $1^{2-}$  as disodium salt.

the protons of the "anthracene" moiety. The low-field proton absorptions which correspond to the "phenanthrene" component appear as two, very broad, unresolved bands centered at 7.6 and 6.4 ppm. A decrease of the sample's temperature caused a concomitant drastic sharpening of the low-field signals. At  $-50$  °C the  $^1\text{H}$  NMR absorptions are quite similar to those exhibited by  $1^{2-}$  dilithium salt (Figure 2, bottom). The changes in the line widths are found to be reversible; i.e., as the sample's temperature is increased, the low-field signals broaden, up to a total disappearance at  $40$  °C. In contrast, the line shapes of the protons assigned to the so-called "anthracene" moiety are almost unaffected by alteration of the sample's temperature; the signals remain sharp and highly resolved. The  $^{13}\text{C}$  NMR spectrum of  $1^{2-}$  disodium salt reveals similar phenomena; i.e., the carbon atoms which constitute the "phenanthrene" moiety (including  $\text{C}_{8b}$  and  $\text{C}_{16a}$ ) reveal broad, almost undetectable signals which sharpen as the sample's temperature is decreased. Thus  $1^{2-}$  disodium salt presents a very clear demonstration of the already mentioned partitioning phenomenon.

**9-(9'-Phenanthryl)anthracene (4) Tetraanion.** The reduction of the 9-(9'-phenanthryl)anthracene system (**4**) was performed with lithium and sodium metals. In the course of the reduction



(2) Young, R. N. *Prog. Nucl. Magn. Reson. Spectrosc.* **1979**, *12*, 261–286.  
 (3) For the  $\pi$ -electron SCF-MO scheme see: Meyer, A. Y. *Theor. Chim. Acta* **1970**, *16*, 226–238. The evaluation of integrals is described in: Meyer, A. Y. *Ibid.* **1968**, *9*, 401–411. The structural parameters of the dianion were obtained from  $\omega\beta$  calculations, as crystallographic data concerning the charged system are unavailable.

process the originally colorless solution, exposed to the lithium wire, turned blue, blue-green, and then brown, with no  $^1\text{H}$  NMR absorptions being observed. Reoxidation at this stage by means of dry oxygen yielded the starting system as sole product. Further

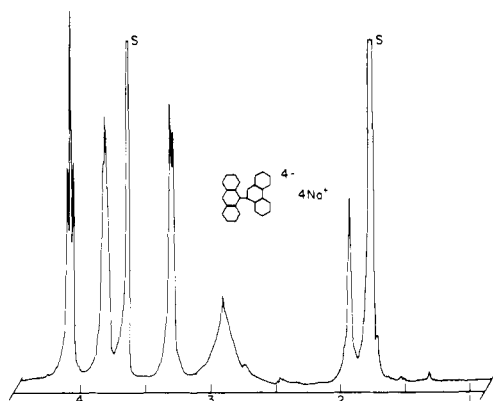


Figure 3.  $^1\text{H}$  NMR spectrum of  $4^{4-}$  as tetrasodium salt ( $-50\text{ }^\circ\text{C}$ ).

exposure to the metal caused a precipitation of a very dark insoluble material; reoxidation of this precipitate resulted in the formation of a black, insoluble compound which could not be identified.

When a THF solution of **4** was treated with sodium metal, a sequence of colors similar to that exhibited during the lithium reduction process was observed. In this case, however, further exposure to the metal did not result in a precipitation; instead, the brown solution turned purple, a process which was accompanied by the appearance of  $^1\text{H}$  NMR absorptions. At room temperature the  $^1\text{H}$  NMR spectrum obtained is composed of three broad, unresolved signals centered at ca. 4.0, 3.2, and 2.0 ppm. Upon cooling, these high-field bands sharpen; yet, even at  $-50\text{ }^\circ\text{C}$  the band-narrowing process is not completed and only three out of the five exhibited absorptions reveal splitting patterns (Figure 3). Decoupling experiments, relative signal intensities, and comparison with the  $^1\text{H}$  NMR spectrum revealed by the bianthryl tetraanion system ( $5^{4-}$ , vide supra) clearly indicate that all the mentioned five signals belong to the protons of the anthracene moiety (4.08 ppm, t,  $\text{H}_{3,6}$ ; 3.80 ppm, br,  $\text{H}_{2,7}$ ; 3.36 ppm, d,  $\text{H}_{4,5}$ ; 2.88 ppm, br,  $\text{H}_{1,8}$ ; and 1.96 ppm, s,  $\text{H}_{10}$ ). No  $^1\text{H}$  NMR absorptions ascribed to the phenanthrene component protons could be detected. A further decreasing of the sample's temperature to  $-80\text{ }^\circ\text{C}$  resulted in the appearance of very broad, unresolved signals at ca. 2.8 and 1.8 ppm, tentatively assigned to protons  $\text{H}_2$  ( $\text{H}_7$ ) and  $\text{H}_3$  ( $\text{H}_6$ ) of the phenanthrene moiety. Increasing the temperature of the sample caused an immediate, total disappearance of the broad bands ascribed to the phenanthrene component protons as well as a considerable broadening of all the other absorptions.

The  $^{13}\text{C}$  NMR spectrum of the sodium reduction product of 9-(9'-phenanthryl)anthracene revealed only four signals (instead of the 22 absorptions expected and, indeed, observed in the  $^{13}\text{C}$  NMR spectrum of the neutral starting material **4**). These four absorptions, which are characterized by poor signal-to-noise ratio even at low temperatures, are assigned to the carbon atoms  $\text{C}_3$  (114 ppm),  $\text{C}_4$  (98 ppm),  $\text{C}_{4a}$  (148 ppm), and  $\text{C}_{10}$  (79 ppm).

Reoxidation of the sodium reduction product of 9-(9'-phenanthryl)anthracene at any of the stages yielded the starting neutral system **4**.

Doubly charged systems, derived from catacondensed benzenoid polycycles such as anthracene (**2**), phenanthrene (**3**),<sup>4</sup> and dibenzotetracene (**1**), may generally be classified as antiaromatic, being  $4n\pi$  peripheral conjugated systems.<sup>1</sup> Obviously, this classification which is based upon the Platt's perimeter model<sup>5</sup> is of intrinsic qualitative nature, as the considerably varying measures of antiaromatic contributions are completely disregarded. This observation emphasizes the relative character related to the antiaromatic notion, a relativeness which is well-known to characterize aromatic polybenzenoid hydrocarbons. Experimental as well as theoretical results point toward the fact that linear acenes

such as anthracene (**2**) or tetracene are less stable than angular species like phenanthrene (**3**) or chrysene.<sup>6,7</sup> This phenomenon is ascribed to large dilution of the aromatic sextet exhibited by linear systems<sup>6</sup> or, alternatively, to a smaller number of  $(4n + 2)$   $\pi$ -electrons conjugated circuits in such species.<sup>8</sup> When the notion of relativeness is applied to antiaromatic contributions sustained in various  $4n\pi$  conjugated systems, an interpretation of the previously described phenomena seems to emerge.

Antiaromatic systems are known to be characterized by relatively narrow energy gaps between their lowest vacant and highest occupied molecular orbitals (LUMO and HOMO, respectively).<sup>9,10</sup> A parallelism may be pointed out between the degree of antiaromaticity, in terms of the system's energy content per electron and the measure of the LUMO-HOMO energy gaps.<sup>10</sup> The smaller the gaps become, the larger the estimated energy of the system, indicating a higher degree of antiaromaticity. The LUMO-HOMO energy separation revealed by phenanthrene dianion is considerably smaller than that estimated for the double charged anthracene (0.231 vs. 0.310  $\beta$  unit, respectively).<sup>10</sup> Thus,  $3^{2-}$  may be considered more antiaromatic than  $2^{2-}$  a result confirmed by other theoretical methods.<sup>11</sup> Hence, **3** seems to have "more to lose" when reduced to  $3^{2-}$  than **2**: the phenanthrene system is more aromatic than the anthracene system (vide infra), and the phenanthrene dianion is more antiaromatic than the dianion derived from anthracene. Indeed, the  $^1\text{H}$  and  $^{13}\text{C}$  NMR patterns revealed by the dibenzotetracene dianion system (**1**)<sup>2-</sup> as the dilithium salt, as well as the theoretical charge densities estimated by the SCF-MO method (Table I), may be interpreted on the basis of the above considerations. *The two negative charges are almost exclusively confined to the less antiaromatic "anthracene" moiety*; its carbons and protons reveal therefore larger high-field NMR shifts caused by a pronounced electronic shielding. Consequently, antiaromatic contributions are minimized.

In a previous study we were able to show that a direct result of the characteristic small LUMO-HOMO energy gaps of  $4n\pi$  conjugated systems is the existence of an equilibrium process between their singlet ground state and a low-lying, thermally accessible, triplet state.<sup>12</sup> The smaller the energy gap, the larger is the concentration of the systems with an excited triplet configuration. The interaction between the two unpaired electron spins and the nuclear spins substantially increases the efficiency of nuclear dipole relaxation mechanisms, thus shortening relaxation times. A broadening of NMR lines up to their total disappearance results. When the  $4n\pi$  antiaromatic systems are charged species, such as  $1^{2-}$ ,  $2^{2-}$ , and  $3^{2-}$ , the state of solvation of their counterions was found to exert a marked effect upon the singlet-triplet equilibrium and hence upon their NMR line shapes. Conditions favoring tight contact ions<sup>13</sup> (i.e., large cations elevated temperatures) shift the equilibrium toward the triplet, as the effect of the tightly held countercations is to further decrease the LUMO-HOMO gaps.<sup>12</sup>

As mentioned, anthracene dianion ( $2^{2-}$ ) is estimated to have a relatively wide energy gap. In such a case the effects due to solvation upon the measure of the LUMO-HOMO gap are relatively negligible. Indeed, the "anthracene" moiety in  $1^{2-}$  is almost unaffected as the reducing agent is altered from lithium metal to sodium or when the sample's temperature is reduced. In contrast, the phenanthrene dianion system ( $3^{2-}$ ) is characterized

(6) Clar, E. "Polycyclic Hydrocarbons"; Academic Press: London, 1964; pp 24-85.

(7) Kruszewski, J. *Pure Appl. Chem.* **1980**, *52*, 1525-1540.

(8) Randić, M. *J. Am. Chem. Soc.* **1977**, *99*, 444-450.

(9) Trost, B. M.; Kinson, P. L. *J. Am. Chem. Soc.* **1974**, *97*, 2438-2449.

(10) Minsky, A.; Meyer, A. Y.; Rabinovitz, M. *Tetrahedron Lett.* **1982**, *23*, 5351-5354.

(11) (a) Randić, M., private communication to M. Rabinovitz. (b) Bates, R.; Hess, B. A.; Ogle, C. A.; Schaad, L. J. *J. Am. Chem. Soc.* **1981**, *103*, 5052-5058.

(12) Minsky, A.; Meyer, A. Y.; Poupko, R.; Rabinovitz, M. *J. Am. Chem. Soc.* **1983**, *105*, 2164-2172.

(13) O'Brien, D. H.; Russell, C. R.; Hart, A. J. *J. Am. Chem. Soc.* **1979**, *101*, 633-639.

(4) (a) Müllen, K. *Helv. Chim. Acta* **1976**, *59*, 1357-1359. (b) Müllen, K. *Ibid.* **1978**, *61*, 1296-1304.

(5) Platt, J. R. *J. Chem. Phys.* **1954**, *22*, 1448-1458.

**Table II.** LUMO–HOMO Energy Gaps Estimated ( $\omega\beta$  Method) for Dianions Derived from Benzenoid Polycycles

dianions	pentacene	tetracene	anthracene	phenanthrene	benzophenanthrene	1,2-benzanthracene	dibenzochrysene
$\Delta^a$	0.448	0.414	0.310	0.232	0.111	0.226	0.193

<sup>a</sup>LUMO–HOMO gaps,  $\beta$  units

by a narrow LUMO–HOMO energy gap and, hence, by severe NMR line broadening, the line shapes being largely affected by solvation conditions. Those patterns are clearly reflected in the “phenanthrene” moiety of  $1^{2-}$ ; its  $^1\text{H}$  NMR absorptions reveal a substantial dependence upon the state of solvation of the counter-ercation. Tight ion pairing conditions (reduction with sodium metal, room temperature) result in total disappearance of the “phenanthrene’s” part of the  $^1\text{H}$  NMR spectrum revealed by  $1^{2-}$  (Figure 2).

These observations lead to the surprising conclusion that the partitioning of  $1^{2-}$  is expressed much more profoundly than just by a simple mode of charge distribution. This partitioning seems to involve the MO’s framework of the dianion; *its result may be visualized as an existence of two, rather than one, molecular orbital systems within  $1^{2-}$ —“anthracene”-like and “phenanthrene”-like frameworks.* Each MO system displays its own independent, characteristic features, expressed here by different charge distribution over the two moieties and, what is even more indicative, by the AO’s coefficients of the HOMO and LUMO of the dianion  $1^{2-}$  (Table I). While in the highest occupied MO the atomic coefficients of those carbon atoms which constitute the so-called “anthracene” moiety are estimated as relatively large, they are found to be considerably smaller in the LUMO. A reverse situation characterizes the AO coefficients of the “phenanthrene” moiety carbons, being small in magnitude in the HOMO and relatively large in the LUMO. In view of these results it might be concluded that while in the ground state most of the negative charge resides upon the “anthracene” moiety, this charge density is shifted toward a “phenanthrene” part when the dianion undergoes an electronic excitation.<sup>14</sup>

The mode of partitioning which characterizes the ground state (and emphasizes the dianionic nature of the “anthracene” moiety) results in a system in which the antiaromatic contributions, imposed by the  $4n\pi$  system, are minimized, a state which leads, in turn, to a smaller energy content. A pronounced localization of the negative charge density over the “phenanthrene” part is related to an increase in the overall energy content of the dianion  $1^{2-}$ . The different charge distribution over the two moieties is convincingly exhibited by the  $^1\text{H}$  and  $^{13}\text{C}$  NMR chemical shifts of  $1^{2-}$  as a dilithium salt. On the other hand, the  $^1\text{H}$  NMR patterns of the disodium salt, as well as the estimated HOMO and LUMO atomic coefficients, seem to indicate that the behavior of the dianion is best interpreted in terms of coexistence of two, rather than one, MO frameworks within  $1^{2-}$ .

These interpretations may as well hold to the phenomena presented by the metal reduction product of the 9-(9'-phenanthryl)anthracene system (**4**). The lithium reduction of 9,9'-bianthryl (**5**) was reported to yield the corresponding tetraanion; its  $^1\text{H}$  NMR patterns support a description of the quadruply charged species as being composed of two noninteracting anthracene dianion units.<sup>15</sup> The lithium metal reduction of **4** affords, as mentioned, a product which does not reveal NMR patterns, a formation which is followed by a precipitation of insoluble, polymeric material. The phenanthrene unit, being more aromatic than anthracene (vide infra) and therefore less prone to lose its aromaticity, renders the reduction process of **4** considerably more difficult compared to the reduction of the binanthryl system (**5**). Consequently, whereas the lithium metal shifts

the reduction process of **5** to afford a quadruply charged species it enables only a threefold reduction of **4**, yielding probably to the tri-anion-radical. The radical system, being a reactive intermediate and paramagnetic, tends to polymerize and does not afford NMR patterns.

In ethereal solvents, which are characterized by low dielectric constants (relative to solvents such as water or DMF), sodium metal acts as a stronger reducing agent than lithium.<sup>12</sup> Thus, when a THF solution of **4** is exposed to a sodium wire, the reduction of 9-(9'-phenanthryl)anthracene proceeds to form the corresponding quadruply charged species, a system in which two negative charges are confined to each of the two moieties. According to the above considerations, the dianionic phenanthrene moiety for which a relatively narrow LUMO–HOMO energy gap is estimated should reveal larger antiaromatic contributions than the doubly charged anthracene unit. Apart from the various measures of antiaromaticity, the different energy gaps of the two doubly charged components are expected to cause a dissimilarity in the extent and direction of the singlet–triplet equilibrium previously described as a characteristic feature of antiaromatic systems. This dissimilarity is unambiguously demonstrated by the  $^1\text{H}$  NMR patterns of  $4^{4-}$  as a sodium salt. At room temperature only broad absorptions are revealed, all of which are assigned to the anthracene unit. As the sample’s temperature is reduced, these  $^1\text{H}$  NMR lines sharpen. However, even at a temperature as low as  $-50^\circ\text{C}$ , only those protons which are farthest from the phenanthrene moiety (i.e.,  $\text{H}_{3,6}$ ,  $\text{H}_{4,5}$ , and  $\text{H}_{10}$ ) attain a fine structure whereas  $\text{H}_{1,8}$  exhibit a very broad, unresolved pattern (Figure 3); the phenanthrene unit protons do not reveal NMR absorptions. Similar results are obtained when the  $^{13}\text{C}$  NMR spectrum of the tetraanion is considered. We may, therefore, assume that while the spectral properties of the dianionic anthracene moiety are determined by a singlet, ground-state configuration, those exhibited by the doubly charged phenanthrene unit are governed by an excited triplet state. The triplet configuration, being paramagnetic, disables any detection of the phenanthrene moiety NMR absorptions. Moreover, it exerts a distance-dependent influence upon the anthracene unit, resulting in  $^1\text{H}$  as well as  $^{13}\text{C}$  NMR line broadening which increases as the nuclei come closer to the phenanthrene moiety. As the sample’s temperature is reduced, line sharpening is observed as the magnitude of triplet, paramagnetic contribution decreases (vide infra).

The described phenomena, revealed by the di- as well as tetraanions derived from dibenzotetracene (**1**) and 9-(9'-phenanthryl)anthracene (**4**) systems, respectively, present an experimental support to the theory and assumptions hitherto based upon purely theoretical considerations<sup>11</sup> concerning the rather elusive nature of antiaromaticity. The interpretation of these phenomena points toward an unequivocal correlation between antiaromaticity and a narrow energy gap between the lowest vacant and the highest occupied molecular orbitals of antiaromatic systems. This narrow gap leads to considerable contributions of a low-lying, excited triple configuration to the overall character of the antiaromatic species. The assignment of a crucial role to these contributions enables a straightforward explanation of spectral phenomena revealed by  $4n\pi$  conjugated polycycles, such as temperature-dependent NMR line broadening. Moreover, the different measures of the triplet state contributions, caused by a different LUMO–HOMO splitting, are expected to result in varying magnitudes of antiaromaticity in the various systems. Theoretical calculations performed on dianions derived from benzenoid polycycles (Table II) indicate that the LUMO–HOMO energy gaps estimated for the linear systems are larger than those obtained for the angular systems. In terms of the estimated LUMO–HOMO gaps, it may be generalized, therefore, that

(14) A referee has suggested an explanation that differs slightly from ours, i.e., that the lowest singlet state is largely localized in the anthracene portion of  $1^{2-}$  and the lowest triple which is an excited state has an appreciable electron density in the phenanthrene portion. However, the MO’s of  $1^{2-}$  support our explanation.

(15) Huber, W.; Müllen, K. *J. Chem. Soc., Chem. Commun.* **1980**, 698–700.

angular  $4n\pi$  conjugated polycycles, exemplified by phenanthrene dianion  $3^{2-}$ , sustain larger antiaromatic contributions than are exhibited by the linear systems. This theoretical-based assumption is now clearly demonstrated experimentally by the anions derived from dibenzotetracene (1) and 9-(9'-phenanthryl)anthracene (4).

### Experimental Section

**Dibenzotetracene (1)** was prepared by a bis-Wittig reaction between phenanthrenequinone and the bis(triphenylphosphine) dibromide salt derived from 2,3-dimethylnaphthalene. The reaction was conducted under phase-transfer catalysis conditions using LiOH as a base.<sup>16</sup>

**9-(9'-Phenanthryl)anthracene (4)** was prepared by a Grignard reaction between 9-phenanthrylmagnesium bromide and anthrone in a mixture of dry benzene and THF. The reaction was conducted at room temperature for 24 h while strict anhydrous conditions and nitrogen atmosphere were maintained.

(16) Minsky, A.; Rabinovitz, M. *Synthesis* 1983, 6, 497-498.

The anionic species were prepared by reduction of the respective neutral compounds with sodium or lithium metals. A wire of the metal was introduced to the upper part of an extended 5-mm NMR tube containing  $10^{-2}$  M of the hydrocarbon dissolved in THF- $d_6$  (Aldrich). The frozen solution was degassed, and then the tube was sealed under vacuum. The solution was brought into contact with the metal for controlled periods by turning the tube upside down.

The NMR spectra were obtained on Bruker WH-300 pulsed FT spectrometer operating at 300.133 and 75.46 MHz for  $^1\text{H}$  and  $^{13}\text{C}$  NMR, respectively, equipped with an Aspect-2000 computer.

**Registry No.** 1, 216-00-2;  $1^{2-}$ , 91586-08-2;  $1^{2-}\cdot 2\text{Li}^+$ , 91586-12-8;  $1^{2-}\cdot 2\text{Na}^+$ , 91586-14-0; 4, 91586-10-6;  $4^+$ , 91586-09-3;  $4^+\cdot 4\text{Na}^+$ , 91606-04-1; Li, 7439-93-2; Na, 7440-23-5; 9,10-phenanthrenequinone, 84-11-7; 2,3-dimethylnaphthalene bis(triphenylphosphonium) dibromide, 39013-98-4; 9-phenanthrylmagnesium bromide, 71112-64-6; anthrone, 90-44-8; pentacene dianion, 34484-46-3; tetracene dianion, 53571-97-4; anthracene dianion, 56481-92-6; phenanthrene dianion, 67382-15-4; 9,10-benzophenanthrene dianion, 66973-59-9; 1,2-benzanthracene dianion, 78858-01-2.

## Ion Pairing and Reactivity of Enolate Anions. 5. Thermodynamics of Ionization of $\beta$ -Di- and Tricarbonyl Compounds in Dimethyl Sulfoxide Solution and Ion Pairing of Their Alkali Salts<sup>1</sup>

Edward M. Arnett,\* Stephen G. Maroldo, Steven L. Schilling, and John A. Harrelson

Contribution from the Department of Chemistry, Duke University, Durham, North Carolina 27706. Received March 23, 1984. Revised Manuscript Received May 25, 1984

**Abstract:** A variety of  $\beta$ -di- and triketones and esters with different substituents and conformations were deprotonated by the potassium salt of  $\text{Me}_2\text{SO}$  in that solvent. Standard free energies, enthalpies, and entropies of ionization are derived from  $\text{p}K_a$ 's and heats of deprotonation. The overall effects of structure variation for the ketones and esters reported here follow generally accepted patterns based on the merged results of many previous studies in various solvents: acyclic ketones are slightly more acidic than analogous esters, cyclic members of both series are more acidic than acyclic analogues, and alkyl substitution on the carbon bearing the acidic proton reduces acid strength while accumulation of carbonyl groups on the acidic carbon increases acidity. These trends are also followed in the gas phase and so are not the result of solvent effects. Although a good extrathermodynamic correlation is found for  $\text{p}K_a$ 's of ketones vs.  $\text{p}K_a$ 's of analogous esters and a fair correlation is found for  $\Delta G_i^\circ$  vs.  $\Delta H_i^\circ$ , an attempted "isoequilibrium plot" of  $\Delta H_i^\circ$  vs.  $\Delta S_i^\circ$  is a virtual random scatter of points. In view of the many stereoelectronic and solvation factors which may be affecting the acidities of these compounds, we have avoided interpreting variations of less than 2 kcal/mol in making comparisons between individual compounds. However, the acidities of the Meldrum acids are so large compared either to acyclic diesters or to analogous dimesones that discussion seems to be justified in terms of Huisgen's analysis of dipole opposition in cis vs. trans ester conformations. Ion-pairing constants ( $K_{\text{assoc}}$ ) for the alkali enolates were obtained for several cases both by conductance and the Bordwell titration method with good agreement in most of those cases studied by both methods. In terms of  $\log K_{\text{assoc}}$ , there is a generally good correlation between the interaction of potassium and sodium ions with the enolate anions reported here, but the lithium ion and the proton ( $\text{p}K_a$ 's) show no correlation with the larger cations. The complexities of this extensive analysis of relatively simple and well-defined enolates provide a warning against the interpretation of relatively small rate or product differences (e.g., <2 kcal/mol) of more complex enolates under less controlled conditions in terms of ad hoc structure-reactivity arguments.

Base-promoted reactions of carbonyl compounds are the largest single class of synthetic processes in organic chemistry.<sup>2-5</sup> One need only consider the many classical variants of aldol chemistry or of its most recent applications to stereochemical control<sup>6-8</sup> to

appreciate the importance of enolates as reactive intermediates. However, there have been a disproportionately small number of systematic studies of enolate reactions from the viewpoint of physical organic chemistry. These have been summarized in several reviews.<sup>9-12</sup>

(1) For previous papers in this series, see: (a) Arnett, E. M.; DePalma, V. M. *J. Am. Chem. Soc.* 1976, 98, 7447. (b) Arnett, E. M.; DePalma, V. M. *Ibid.* 1977, 99, 5828. (c) DePalma, V. M.; Arnett, E. M. *Ibid.* 1978, 100, 3514. (d) Arnett, E. M.; DePalma, V.; Maroldo, S.; Small, L. S. *Pure Appl. Chem.* 1979, 51, 131-37.

(2) House, H. O. "Modern Synthetic Reactions"; W. A. Benjamin: Menlo Park, CA, 1972; Chapters 9-11.

(3) Stowell, J. C. "Carbanions in Organic Synthesis"; Wiley: New York, 1979.

(4) Gutsche, C. D. "The Chemistry of Carbonyl Compounds"; Prentice-Hall: Englewood Cliffs, NJ, 1967.

(5) *Org. React. (N.Y.)* 1968, 16, 1.

(6) (a) Evans, D. A. *Aldrichimica Acta* 1982, 15, 23. (b) Evans, D. A.; Nelson, J. V.; Taber, T. R. *Top. Stereochem.* 1982, 13, 1.

(7) (a) Heathcock, C. H. *Science (Washington, DC)* 1981, 214, 395. (b) Heathcock, C. H. In "Comprehensive Carbanion Chemistry", Durst, T., Ed.; Elsevier: Amsterdam, 1983; in press.

(8) House, H. O.; Crumrine, D. S.; Teranishi, A. Y.; Olmstead, H. D. *J. Am. Chem. Soc.* 1973, 95, 3310.

(9) Jackman, L. M.; Lange, B. C. *Tetrahedron* 1977, 33, 2737.

(10) Reutov, O. A.; Kurts, A. L. *Russ. Chem. Rev. (Engl. Transl.)* 1977, 46, 1040.